FINDING THERMAL DISTRIBUTION IN THE CASTING OF AL-ALLOY BY SIMULATION USING FDM.

Ass.Pro. Dr. Adnan Sh. Jabur
College of Engineering
University of Basrah

Heider. Y. Thamir
College of Engineering
University of Al-Qadisiya

Abstract

The object is to get simulated observation of the solidification front movement inside casting, which was extracted from theoretical simulation of the solidification process, in the prediction of shrinkage cavities locations in the final ingots. A (Fortran) program was developed using the finite difference method. Several factors were taken into consideration in this system, such as the variation of liquid and solid volume fractions during solidification, changing the thermophysical properties of the cast metal with changing metal state and temperature. Also, the latent heat was introduced as an isolated source term to the mentioned equation. The verification of the system efficiency was achieved by the comparison between the cavity location in theoretical and real casting. There was a good agreement. Finally, the simulated cooling curves of selected points inside the casting were studied.

Key Words: casting, simulation, solidification, thermal distribution, shrinkage

إيجاد التوزيع الحراري في مسبوكة ألمنيوم بواسطة المحاكاة باستخدام طريقة الفروقات المحددة

د. عدنان شمخي جبر
كلية الهندسة
جامعة البصرة

حيدر ياسر ثامر
كلية الهندسة
جامعة القادسية

الخلاصة

الهدف من البحث هو الحصول على نظرة لتحرك أوجه(أسطح)التجمد داخل المسبوكة من خلال عملية محاكاة نظرية لعملية التجمد باستخدام لغة(فورتران)، للتنبؤ بمواقع الفجوات في المسبوكات النهائية. هناك عدة عوامل أخذت بنظر الاعتبار في هذا النظام منها: التغير في الكسر الحجمي للسائل والصلب إثناء التجمد، والتغير في الخواص الحرارية للمسبوكة مع تغير حالة المعدن ودرجة الحرارة. كذلك فإن الحرارة الكامنة للإنجماد تم إضافتها للمعادلة ضمن النظام. التحقق من كفائة النظام تم بمقارنة النتائج النظرية مع المسبوكة الحقيقية، حيث كان هناك تطابق جيد. وتم دراسة مجموعة من منحنيات التبريد المستحصلة نظريا لنقاط داخل المسبوكة.

Literature Review

Since last three decades using of programming entered to casting filed (design and analyses). The available of high speed processors helped in developing a new programs and packages used in this purpose. Niyama et al (1981), made a mapping of the calculated heat gradient at the time of solidification of large steel casting, and they found that it was a powerful tool for predicating shrinkage porosities, particularly those occurring along the centerline of the casting. They have found that the porosities were formed in those areas where the G at the time of solidification was to be below 2-3 c/cm. Balcar et al(2007), used (MAGMA) software to model the casting and solidification of ingots for open-die forgings to fined directional solidification, grain size, chemical heterogeneity and discontinuities. Vassiliou et al (2008), obtained realistic results from casting simulation programs to the enhancement of process of Centrifugal casting. Charach and Zarmy (1991), proposed an analytical solution for planar solidification in a finite thickness slab by transforming the problem to one without the density change. Huang and Akay(1995), studied a heat transfer phenomena at cast-mold interface. Trovant and Argyropoulos(1996), proposed an algorithm to account for shrinkage and consequently determine the shrinkage profile resulting from phase and density change. Campell and Wright(1997), improved using of cooling fins by simulation of solidification and calculate solidification time. Qasssim Daws(1997), developed a program for steel castings solidification and derived an equation to calculate a less length of runner. Yapping (1999), simulated a continuous casting for large aluminum castings by finite element method to locate hot spot and analyze thermal stresses. Bounds et. al.(2000), proposed a model for macro defect predictions based on the coupling of the free-surface flow, heat transfer, and solidification.

Experimental Procedure of Work

1- Materials and instruments

The materials, tools and instruments which are used in the present work are:

1- One kilogram of Aluminum alloy of type LM13 with a standard chemical composition contained in **Table (1).**
2- An alumina crucible.
3- A wood pattern of the ingot with dimensions as shown in **Figure (1).**
4- A sand mold with a dimensions (30× 40× 40 cm).
5- A gas furnace for melting.
6- Degasser of type (C_2Cl_6), for the melt degassing.
7- K-type thermocouple with a digital thermometer.

Al	Cu	Fe	Mg	Ni	Si
84.3	0.9	0.8	1.2	0.8	12

2-

Casting procedure

The melting procedure of the alloy was accomplished by using the gas furnace. After the molten alloy reaches (620^{o}C) it was degassed, then the crucible is removed from the furnace, and preparing for pouring at (610^{o}C). The temperature control was achieved by using the thermocouple.

3- Cavities localization

After the solidification is completed, the sand mold is broken, and the ingot was left to cool. Then it was sectioned longitudinally through the two perpendiculars mid planes. Then other sections were done to precisely identify the cavities extension, **Figure (2).**

4- Numerical Modeling

1- Assumptions Made

The following assumptions were made for the formulation of the problem;

1. Mold is filled instantaneously.
2. Phase transformation proceeds in one direction: liquid to solid.
3. No convection is present in the liquid metal.
4. Initially the molten metal is at a uniform temperature.

2- Solid fraction and latent heat

The latent heat was added to the model as a source term. The following processing shows this treatment(Xue,1991):

$$\rho.c(\frac{\partial T}{\partial t}) = K(\frac{\partial^2 T}{\partial x^2} + \frac{\partial^2 T}{\partial y^2} + \frac{\partial^2 T}{\partial z^2}) + Q^{\bullet} \qquad \text{…….1}$$

$$\rho.c(\frac{\partial T}{\partial t}) = K(\frac{\partial^2 T}{\partial x^2} + \frac{\partial^2 T}{\partial y^2} + \frac{\partial^2 T}{\partial z^2}) + \rho.L.\frac{\partial f_S}{\partial t} \qquad \text{……..2}$$

$$\frac{\partial f_S}{\partial t} = \frac{\partial f_S}{\partial T}.\frac{\partial T}{\partial t} \qquad \text{……..3}$$

$$\rho.c(\frac{\partial T}{\partial t}) = K(\frac{\partial^2 T}{\partial x^2} + \frac{\partial^2 T}{\partial y^2} + \frac{\partial^2 T}{\partial z^2}) + \rho.L.\frac{\partial f_S}{\partial T}.\frac{\partial T}{\partial t} \qquad \text{…..……4}$$

$$\rho.c(\frac{\partial T}{\partial t}) - \rho.L.\frac{\partial f_S}{\partial T}.\frac{\partial T}{\partial t} = K(\frac{\partial^2 T}{\partial x^2} + \frac{\partial^2 T}{\partial y^2} + \frac{\partial^2 T}{\partial z^2}) \qquad \text{…….5}$$

$$\frac{\partial T}{\partial t}(1 - \frac{L}{c}.\frac{\partial f_S}{\partial T}) = \frac{K}{\rho.c}(\frac{\partial^2 T}{\partial x^2} + \frac{\partial^2 T}{\partial y^2} + \frac{\partial^2 T}{\partial z^2}) \qquad \text{……6}$$

For simplicity, it was supposed that solidification process is linear with decreasing temperature, so the rate: $\frac{\partial f_S}{\partial T}$ can be approximated as:

$\frac{\partial f_S}{\partial T} = 1 - \frac{T - T_{solidus}}{T_{Liquidus} - T_{solidus}}$, and the above equation becomes:

$$\frac{\partial T}{\partial t} = \frac{K}{\rho.c}\left(\frac{\partial^2 T}{\partial x^2} + \frac{\partial^2 T}{\partial y^2} + \frac{\partial^2 T}{\partial z^2}\right) \frac{1}{[1 - (1 - \frac{T - T_{solidus}}{T_{Liquidus} - T_{solidus}}).(\frac{L}{c})]} \qquad \text{……..7}$$

5- System Thermophysical Properties

The thermophysical data can be classified into three classes: temperatures which are used to control the display options, the thermal properties which are used to solve the energy equation; and the phase change properties which are used to convert the specific heat content of each cell to its representative temperature.

1- Thermophysical properties of the sand

The thermal properties of the mold sand remain constant during casting process. They are(Mills,2002):

Initial temperature, $T = 30^{\circ}$C

Density, ρ = 1500 Kg/m^3

Thermal conductivity, K = 0.5 W/m .C

Specific heat, C = 666 J/Kg.C

2- Thermophysical properties of the alloy

The aluminum alloy properties were changed with respect to state of casting (liquid or solid), these are thermal conductivity and heat capacity, while the density value was changed with respect to temperature change using a linear relationships at liquid state and solid state. (Mills,2002)

1- Liquid state

Temperature of pouring, $T_P = 610^{\circ}$C

Liquids temperature, $T_L = 573^{\circ}$C

Density, ρ= 2482-0.27×(T- T_L) Kg/m^3 ……..8

Thermal conductivity, K = 64 W/m .C

Specific heat, C = *1200* J/Kg.C

2- Solid state (Mills,2002)

Solidus temperature, $T_S = 542^{\circ}$C

Density, ρ = 2690-0.19×(*T-25*) Kg/m^3 …….9

Thermal conductivity, $K = 160$ W/m .C

Specific heat, C = 1000 J/Kg.C

3- Mushy state

In the mushy state any thermophysical property is treated according to rule of mixture, where required property (P) can be calculated at temperature T from Equation 10, where $f_{s\,(T)}$ is the solid fraction at T and P_S and P_L are values of the property at the solid and the liquid state, respectively.[11]

$$P_T = f_{s\,(T)}\,P_S + (1 - f_{s\,(T)})P_L \qquad \ldots\ldots\ldots\ldots 10$$

Latent heat, L = 489000 J/Kg

Mushy temperature interval, $\Delta T = 31$

6- Finite Difference Formulation

According to the method of finite difference formulation the differential equation can be formulated as:

$$T_{x,y,z}^{t+\Delta t} = T_{x,y,z}^{t} + \left[\frac{\alpha \Delta t}{\left[1-(1-\frac{T-T_{solidus}}{T_{Liquidus}-T_{solidus}}).(\frac{L}{C})\right]}.\left(\frac{T_{x+1}^{t}-2T_{x}^{t}+T_{x-1}^{t}}{(\Delta x)^2}+\frac{T_{y+1}^{t}-2T_{y}^{t}+T_{y-1}^{t}}{(\Delta y)^2}+\frac{T_{z+1}^{t}-2T_{z}^{t}+T_{z-1}^{t}}{(\Delta z)^2}\right)\right]$$

where:

$\alpha = \dfrac{K}{\rho.C}$, which is called the thermal diffusivity.

7- Casting System Meshing

The casting system (mold and ingot) were divided into 384000 cubes with a dimensions of (0.5 × 0.5 × 0.5 cm). The ingot consists of (1680) cubes, (**Figure 3**). To clarify the solidification front by contours progress, the shape of ingot was sectioned into six layers (A, B, C, D, E, and F) with (0.5 cm) thickness, each layer consists of (280) meshes, (**Figure 4**). The solidification contours are drawn on these slides.

8- Computer Working

1- Time-Step

The time-step can either be defined by the user, or calculated by the Euler stability law. The time-step used in program is (0.05 sec), and the total steps are (12000) steps, that means the total time of program is (600) seconds.

2- Programming

Using the Fortran Language (FORTRAN POWER STATION ©1995) the program was made to use in this work to apply analytical solutions for each mesh in the system (mold and cast) to solve equations which are related to the case. The program deals with each mesh as is it sand or cast? Then with the cast as is it liquid, solid, or mushy? Then gives each case its specified properties but with mushy state it calculates the solid fraction and adds the latent heat of solidification to heat transfer equation with respect to solid fraction. Finally the program print results at all time steps.

Results and Discussion

1-Simulation Verification

Figure (5) contains a photograph of ingot slices with a simulated cavity prediction at one of the final stages for comparison and to verify the system efficiency in identifying the shrinkage cavities locations. From this comparison , it was found that the simulation coincides approximately with real casting in the allocation of the shrinkage cavity through x-axis and its deviation far to the fin near to the other side. This was explained by the chilling effect of the fin at the solid state . But the real cavity appeared divided into two parts. This may be due to the bad mold preparation and uneven ingot thickness. Also, the simulation succeeded in the cavity prediction through y-axis, so the cavity is symmetric in this axis. On the other hand, the cavity simulation did not coincide with real casting through z-axis because the real cavity deviated to the bottom part of the ingot, while it is symmetric in simulation. This is due to ignoring the effect of the sprue which was attached to the lower part of the ingot by a gate which partially played a role of feeder, consequently pulling the cavity down.

2- Simulation of Solidification

Only the solidification front movement of the three layers A ,B, and C will be studied in this paragraph because the ingot was considered symmetric through z-axis , so that the solidification mechanism in these layers is same as that of D ,E , and F layers . The three states of metal were defined by three colors. The red defined the full liquid state (higher than 573 $^{\circ}$C), the yellow defined the mushy (liquid + solid) state (between 573 and 542 $^{\circ}$C), and the blue defined the full solid state (lower than 542 C). The most important indications which can be summarized from the simulation stages **(Figure 6**) are:

-At second (3) after pouring, the transformation from liquid to mushy state , initiated at the layer (A) in the first two cubes at the fin edge toward the other side in the x-direction, while this transformation in (B and C) layers occurred in a thickness of one cube in x-direction .This change continued at second (4) and the next time with different speeds depending on the distance between the layer and the lower surface . The solidification starting at the fin edge is an expected behavior because it has a high area/volume fraction.

-At second (4), the solidification also started at the four corners of ingot. This event occurred at second (7) for (B) and (C) layers.

-At second (10), the transformations of the fin and the surrounding of ingot for three layers were completed.

-At second (14), the transformation of layer (A) was completed and the other layers continued changing.

-At second (18), the liquid/mushy change for three layers was completed.

-From seconds (18) to (85.1), it was indicated that, the metal remained for a long time at the mushy state. This was an expected behavior, because the cooling rates decreased at the solidification range due to the evolution of the latent heat.

-When watching the liquid/mushy changing through 4 , 7 , 10 , and 14 seconds, it was noted that the mushy region was located at the center of ingot ,which means that there is no chilling effect on the fin because the liquid and mushy states have low conductivity .

-At second (85.1), the mushy/solid change started at the fin edge with the same differential in speed between the three layers .

-At second (429.05), the enclosing of the solidification loops in layers (B) and (C) completed.

-The most important indication was that, the cavity position deviated from the center of ingot toward the other side of fin .This can be attributed to the role of the fin as a chiller due to its high thermal conductivity.

3- Cooling Curves

When the comparison between the cooling curves of points 1 and 2 (**Figures 7 and 8**) were made, it was found that the curve of point 2 showed a steep change in slope after solidification completion, while the curve of point 1 had a gradual transition which can be explained by the heat evolution from the solidification near the fin .Generally, both two cubes had a long time of solidification due to the high heat content of the adjacent liquid ingot.

Points 3, 4, and 5 showed high cooling rates during solidification and a short period of solidification. These were due to the fin nature of thinning and low heat content. Also appeared, the effect of the heat content of the ingot, on the curve of point 5 after solidification, in decreasing the slope (concave).

Between the internal points (6, 7, and 8) ,point 6 has highest cooling rate during solidification , and this is attributed to the effect of near fin which play the role of chiller after changing to solid . This effect decreased with points 7 and then 8 according to the distance between them and the fin.

Conclusions and Suggestions

- **Conclusions**

From the present work, the most important conclusions are

1- The identification of the shrinkage cavities locations can be accomplished by drawing the solidification contours. The appearance of a closed loop in the solidification time contours is the criterion for this type of shrinkage.

2- The difference of the thermal properties between liquid and solid give an influence to change the whole solidification behavior and then the location and extension of shrinkage cavity.

- **Suggestions**

The main suggestions for future work are:

1. The development of the system to predict the cavities extension.
2. Addition of the effect of the pouring system such as sprue and gate to system.

References

1. 1- E. Niyama, T. Uchida, M. Morikawa and S. Saito, "Predicting Shrinkage in Large Steel Castings From Temperature Gradient Calculations", AFS Int. Cast Metals Journal, vol 6, pp 16-22, 1981.
2. 2- Martin.L. Balcar, "Modelling of thr Solidification Process and the Chemical Heterogenity of a 26NiCrMoV115 Steel Ingot "Materials and technology, vol 41, PP 139–144, 2007.
3. 3- A. N. Vassiliou"Investigation of Centrifugal Casting Conditions Influence on Part Quality" 3rd ICMEN,PP 347-356, 2008.
4. 4- C. Charach and Y. Zarmi, "Planar Solidification In A Finite Slab; Effect Of Droplet Impact", J. Appl. Phys. Vol.70, pp. 6687-6693, 1991
5. 5- Huang.H, Gurdogan.O, Akay.H.U "Thermal Transport Phenomena in Metalcasting" Simulation AFS Transaction 95 AFS USA 1995 PP 243-246
6. 6- M. Trovany and S. A. Argyropouos, "Mathematical Modeling and Experimental Measurement Of Shrinkage In The Casting Of Metals", Canadian Metallurgical Quarterly, Vol.35, pp 77-84, 1996.
7. 7- Wright .T.C, Campell.J , "Enhanced Solidification Rate in Casting By the Use of cooling Fins", AFS Transaction ,Vol .104 ,AFS USA 1997.PP.639-644.

8. 8- Daws.Q, "Computer Simulation in mould Design ", Ph.D., University of Baghdad, College of Engineering, Iraq, 1997 PP32
9. 9- Yaping.wu "Numerical of Direct – Chill Casting of Aluminum Ingot", PH.D, West Virginia University, College of Engineering and Mineral, 1999.
10. 10- S. Bounds, G. Moran, K. Periclerous, M. Cross, and T.N. Croft: Metall. Mater. Trans. , B, Vol 31B, pp.515-527, 2000.
11. 11- Kenneth C Mills, "Recommended Values of Thermophysical Properties for Selected Commercial Alloys". Woodhead Publishing Limited: Cambridge England 2002.
12. 12- X. Xue, "Modelling and simulation of fluid flow and heat transfer in mold filling". PhD thesis, Technical University of Denmark (1991).
13. 13- J. Gerin Sylvia, "Cast Metals Technology", Addison-Wesley Publishing Company, Inc. USA 1972.

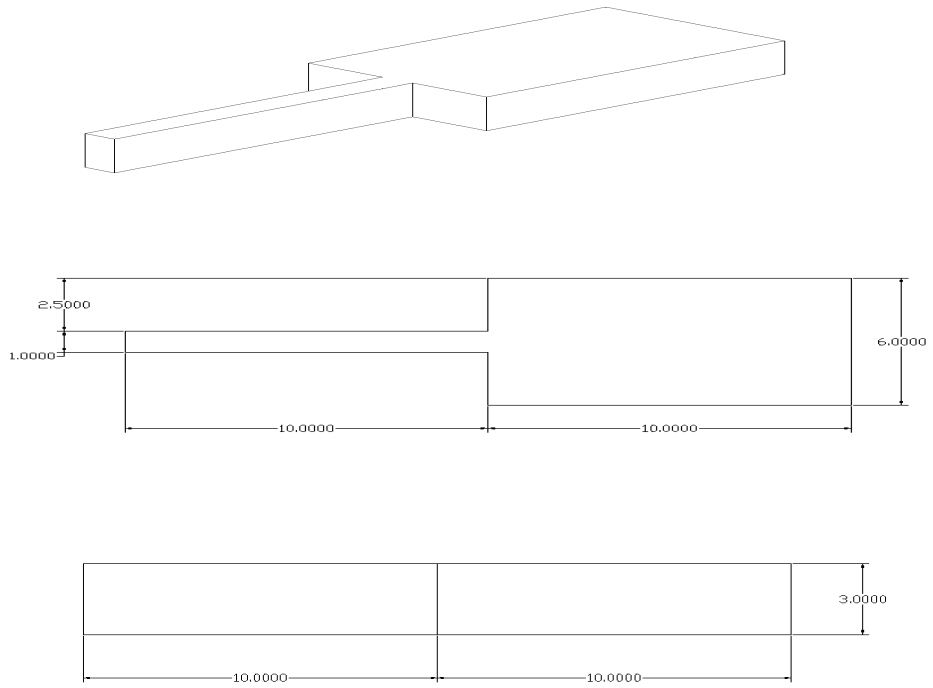

Figure (1) Dimensions of the ingot in (cm)

Figure (2) the cavities

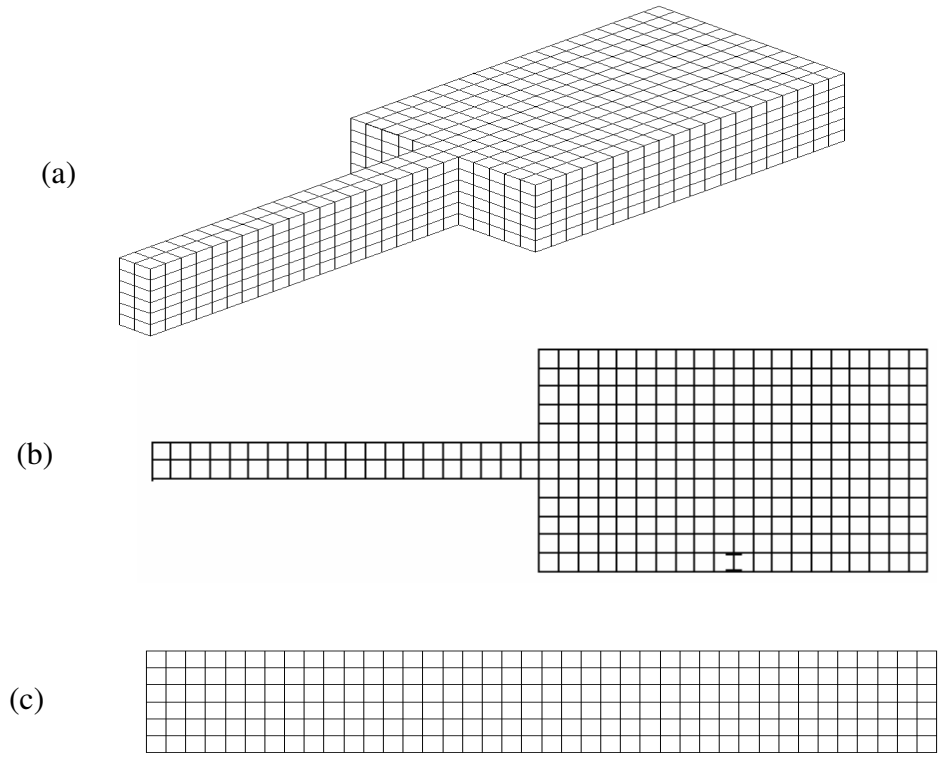

Figure (3) Ingot meshing, a-isometric b-top view, c-side view

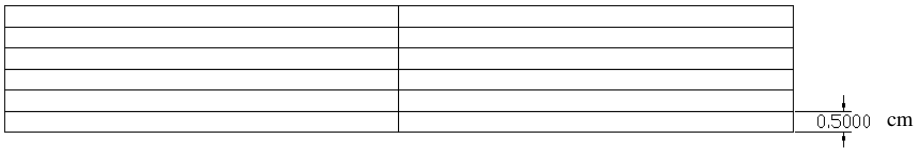

Figure.4. Side view of casting sectioned to layers, A, B, C, D, E and F

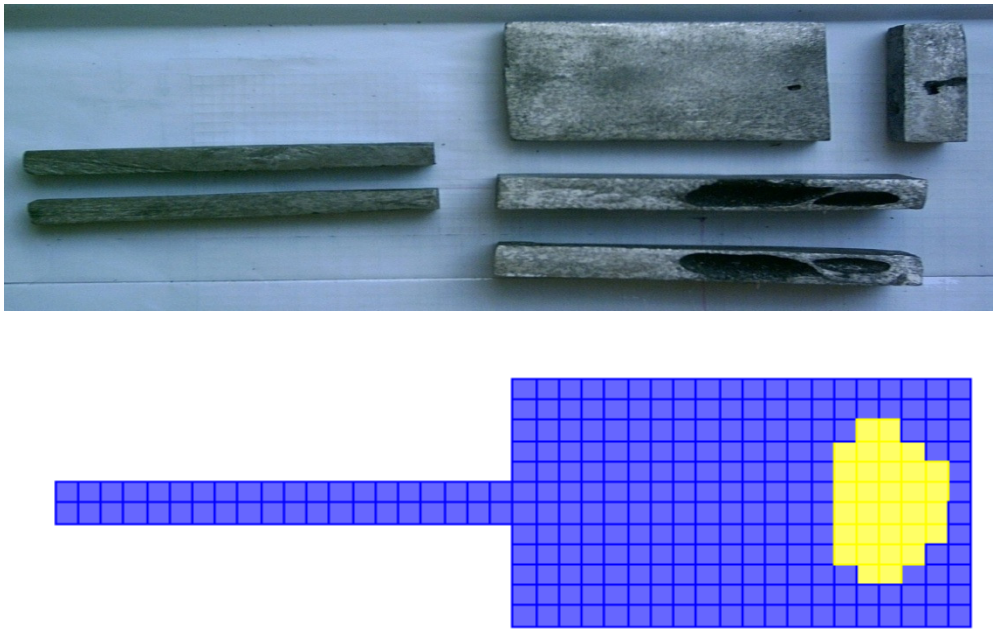

Figure (5) Comparison of photograph of an ingot slices with a simulated cavity prediction

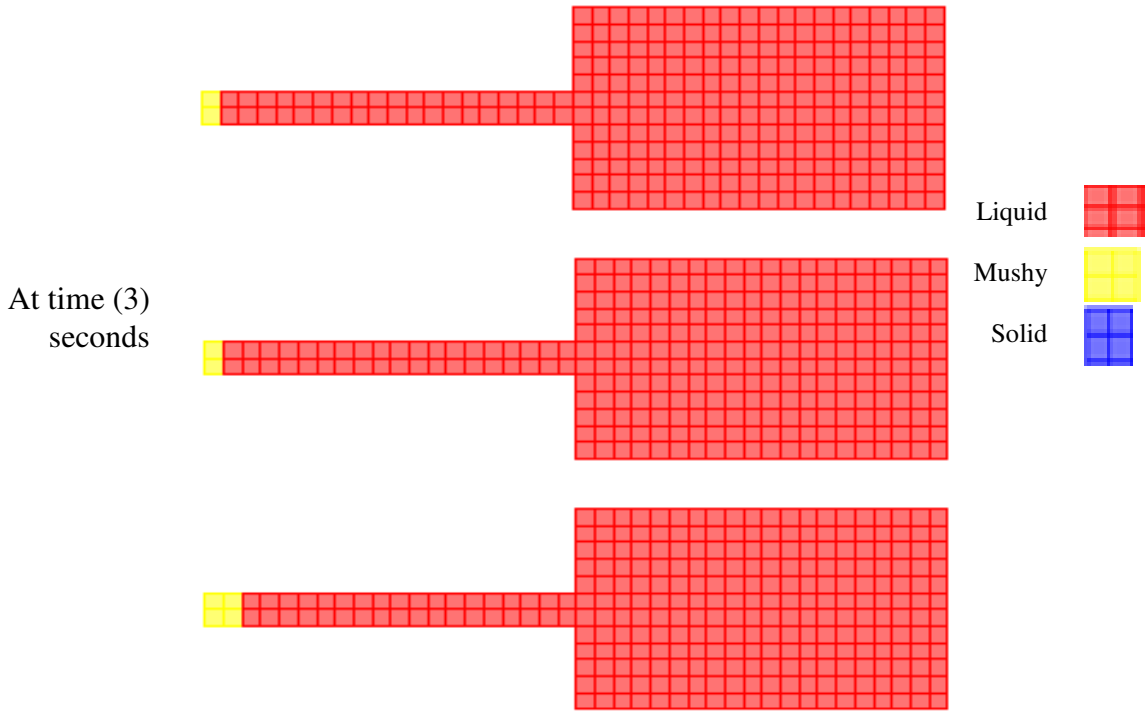

Figure (6) the solidification simulation steps(continue.)

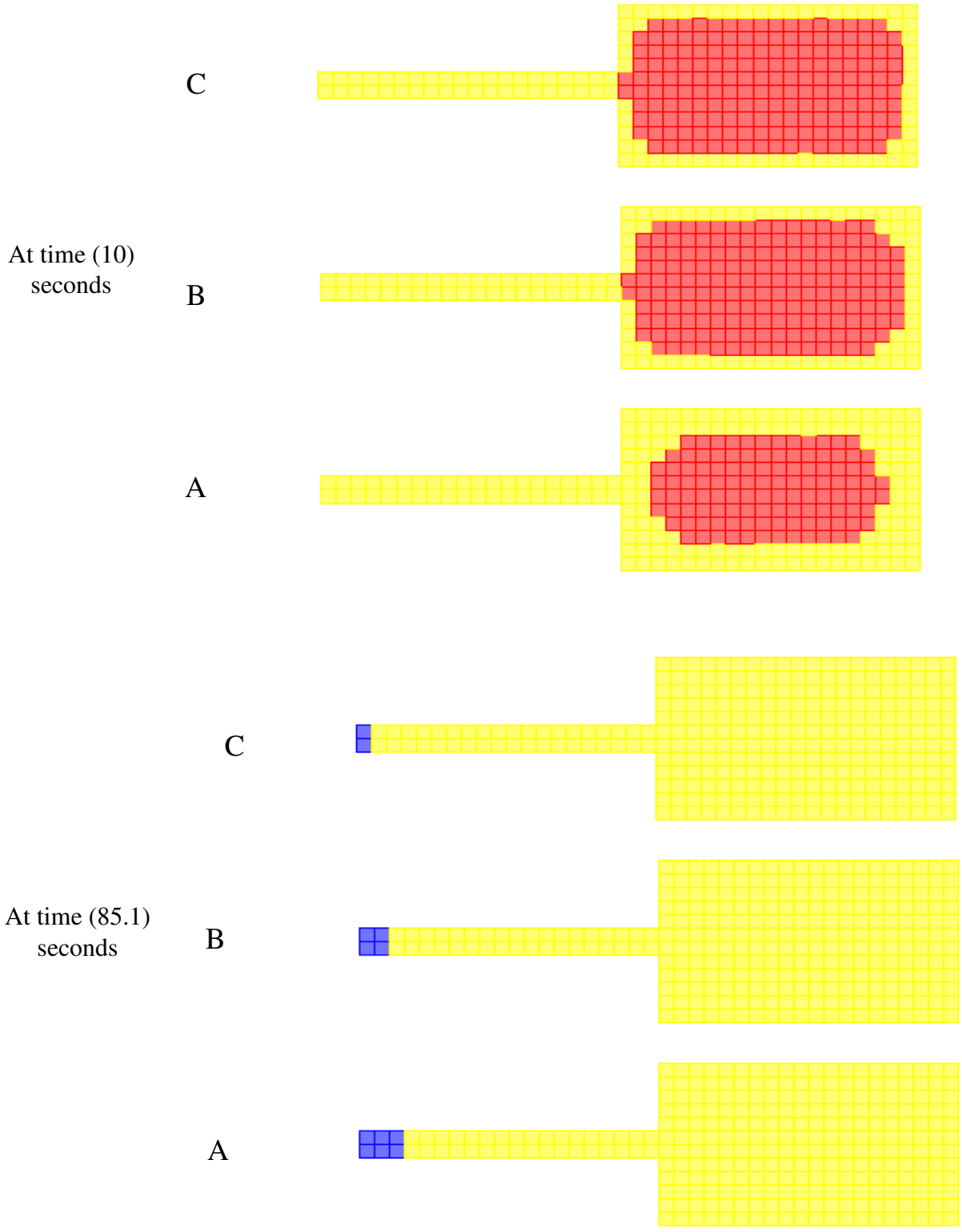

Figure (6) The solidification simulation steps(continue.)

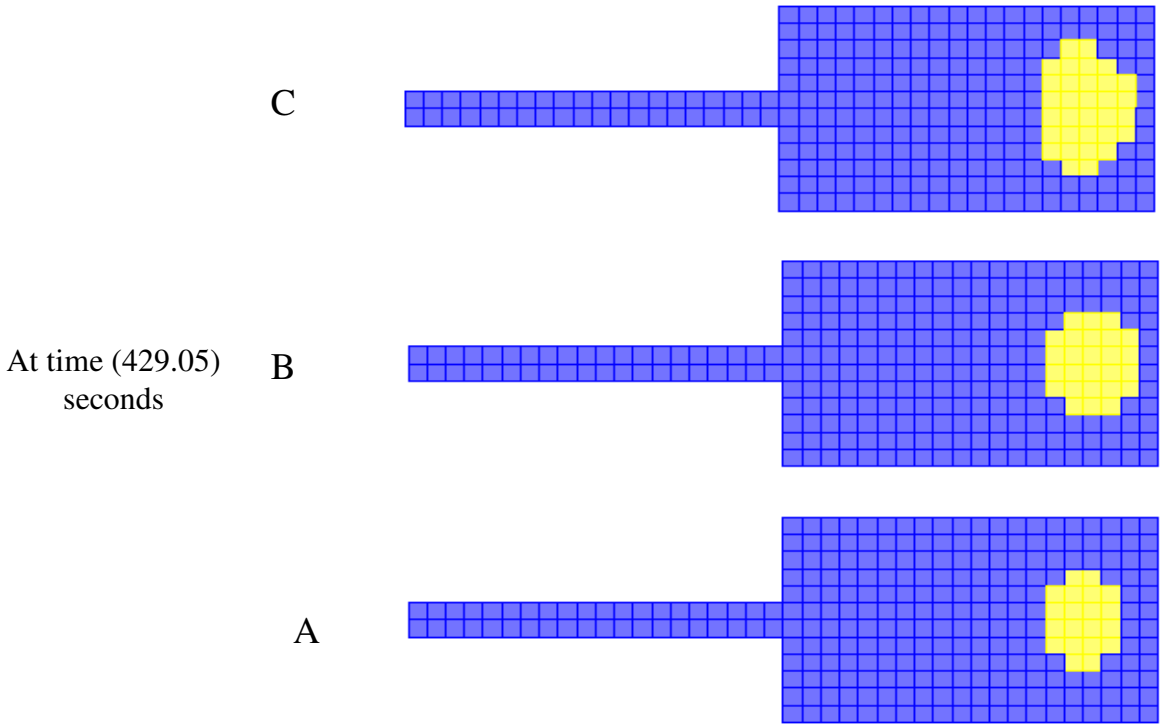

Figure (6) The solidification simulation steps.

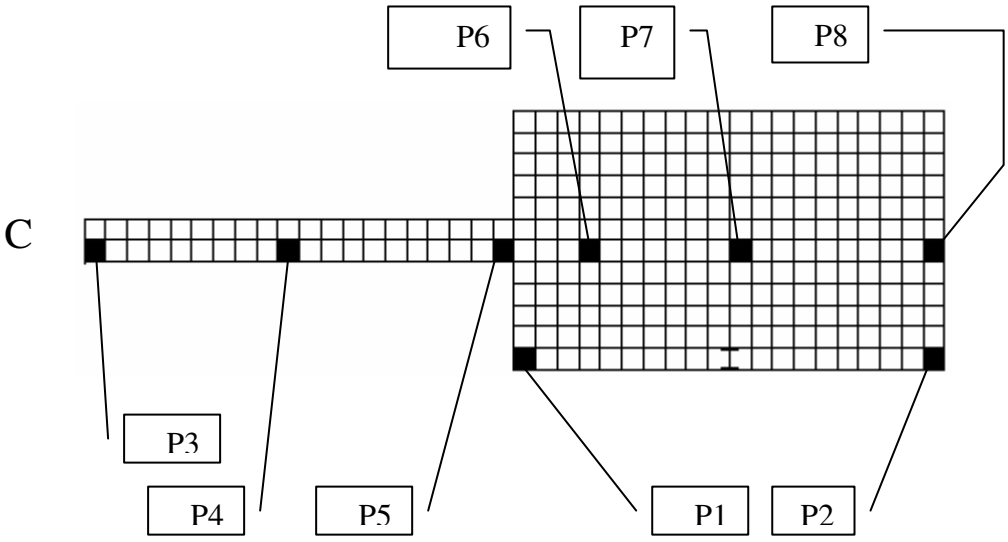

Figure (7) selected points in slice (C)

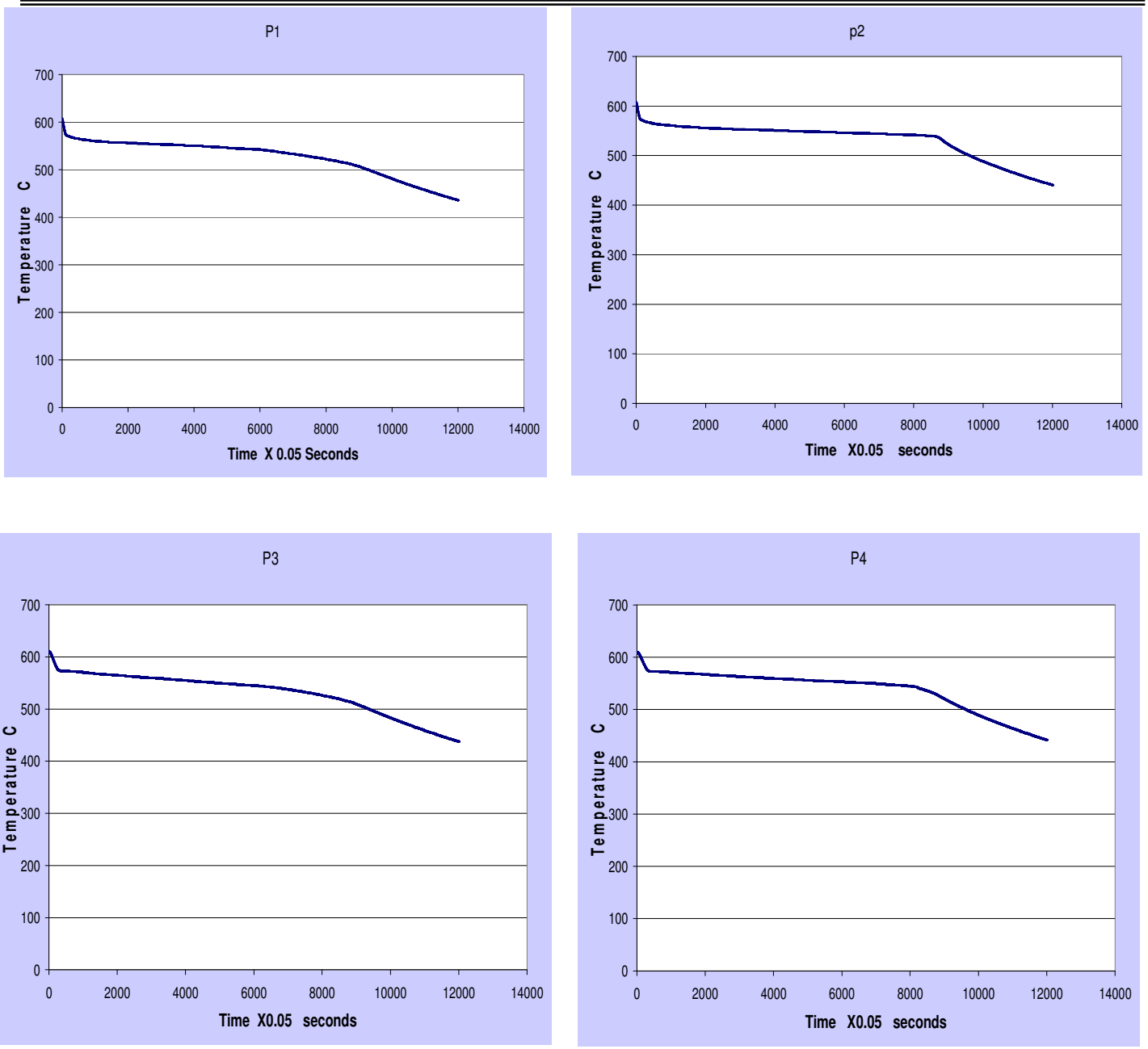

Figure (8) the cooling curves of selected points in the casting (in -C- layer) continue

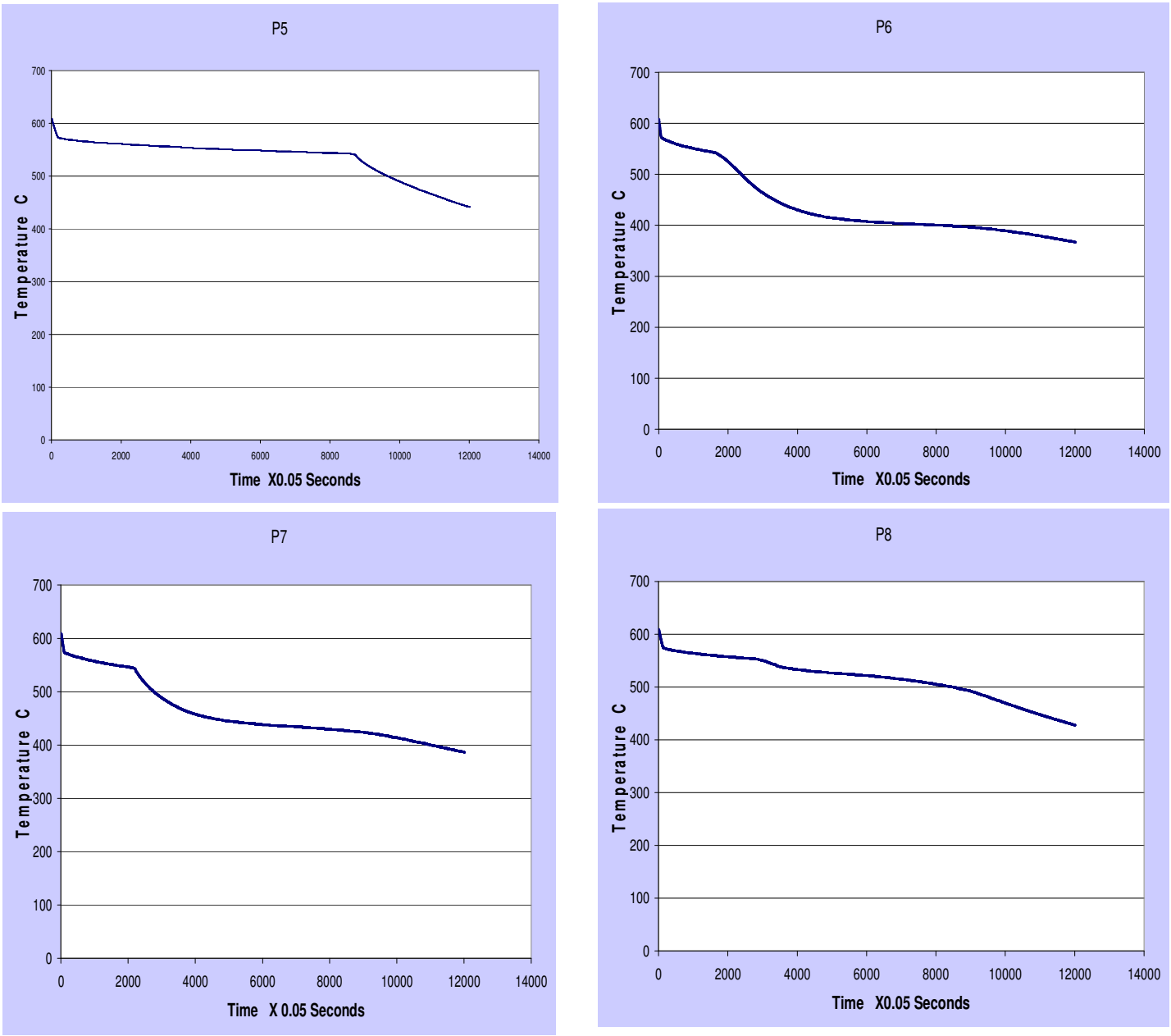

Figure (8) the cooling curves of selected points in the casting (in -C- layer)